Research Article/Araştırma Makalesi

Gazi AKADEMİK YAYINCILIK

GAZİ
JOURNAL OF ENGINEERING SCIENCES

Lightweight Periodic Vibration Isolator Design via Compliant Inertial Amplification Mechanisms with Stiffness Maximized Topologies

Osman Yüksel*[a], Erol Türkeş[b]

Submitted: 28.11.2023 Revised: 20.04.2024 Accepted: 25.04.2024 doi:10.30855/gmbd.0705N13

ABSTRACT

As a novel innovative approach in the literature, periodic structures can be utilized as vibration isolators. In this paper, vibration isolation performance of a lightweight periodic structure is studied. The periodic structure is formed by using inertial amplification mechanisms with stiffness maximized topologies. First of all, inertial amplification concept is introduced on a lumped parameter model. Then, a compliant inertial amplification mechanism, which is the repetitive building block of the periodic structure (i.e., unit cell), is presented. Topology optimization is conducted on this mechanism to attain a stiffness maximized unit cell with reduced weight. After that, a one-dimensional periodic structure is constructed by attaching the lightweight inertial amplification unit cells with stiffness maximized topologies to each other. Finally, vibration isolation performance of the constructed periodic structure is demonstrated via transmissibility plots. It is observed that the designed topologically optimized lightweight periodic structure provides high performance vibration isolation for a wider frequency range with the same stiffness value and less weight, compared to the original structure.

Keywords: Compliance minimization, inertial amplification, periodic structure, topology optimization, vibration isolator

[a,*] Kırklareli University, Faculty of Engineering, Dept. of Mechanical Engineering 39010 - Kırklareli, Türkiye
Orcid: 0000-0001-9492-1756
e-mail: osmanyuksel@klu.edu.tr

[b] Kırklareli University, Faculty of Engineering, Dept. of Mechanical Engineering 39010 - Kırklareli, Türkiye
Orcid: 0000-0002-9601-7119
e-mail: erol.turkes@klu.edu.tr

*Corresponding author: osmanyuksel@klu.edu.tr

Direngenliğin Maksimize Edildiği Topolojilere Sahip Esnek Atalet Artırımı Mekanizmaları ile Düşük Ağırlıklı Periyodik Titreşim Yalıtıcısı Tasarımı

ÖZ

Periyodik yapıların titreşim yalıtıcısı olarak kullanılması son zamanlarda literatürde karşılaşılan yenilikçi bir yaklaşımdır. Bu makalede, düşük ağırlıklı bir periyodik yapının titreşim yalıtımı performansı çalışılmıştır. Periyodik yapı, direngenliğin maksimize edildiği topolojilere sahip atalet artırımı mekanizmaları kullanılarak oluşturulmuştur. İlk olarak, atalet artırımı kavramı toplu parametreli bir model üzerinde tanıtılmıştır. Ardından, periyodik yapının tekrar eden yapı bloğu (birim hücre) olan esnek bağlantılı bir atalet artırımı mekanizması sunulmuştur. Direngenliğin maksimize edildiği düşük ağırlıklı bir birim hücre elde etmek için, bu esnek bağlantılı mekanizma üzerinde topoloji eniyilemesi gerçekleştirilmiştir. Daha sonrasında, direngenliğin maksimize edildiği topolojilere sahip bu düşük ağırlıklı atalet artırımı birim hücreleri birleştirilerek bir boyutlu periyodik bir yapı elde edilmiştir. Son olarak, titreşim iletkenliği grafikleri vasıtasıyla, oluşturulan periyodik yapının titreşim yalıtımı performansı gösterilmiştir. Tasarlanan topolojik olarak eniyilenmiş düşük ağırlıklı periyodik yapının, aynı direngenlikteki eniyileme yapılmamış orijinal yapıya nazaran, daha düşük bir ağırlık ile çok daha geniş bir bant aralığında yüksek performanslı titreşim yalıtımı sağladığı saptanmıştır.

Anahtar Kelimeler: esneklik minimizasyonu, atalet artırımı, periyodik yapı, topoloji eniyilemesi, titreşim yalıtıcısı

To cite this article: O. Yuksel and E. Turkes, "Lightweight Periodic Vibration Isolator Design via Compliant Inertial Amplification Mechanisms with Stiffness Maximized Topologies", *Gazi Journal of Engineering Sciences*, vol.10, no.1, pp. 155-171, 2024. doi:10.30855/gmbd.0705N13

1. Introduction

Achieving vibration control is crucial for mechanical and/or civil engineers, since uncontrolled excitations can result in catastrophic failure situations such as broken apart machine parts and collapsed mechanical structures. In order to mitigate undesired oscillations, active [1-6] and passive [7-11] vibration control methods can be employed. Active control methods require power sources and controllers to deal with mechanical oscillations. On the other hand, propagating waves can be isolated or absorbed by means of passive methods, without employing any electronic device, power source and circuit.

As a subgenre of passive methods, in vibration isolation technique, excitation source and target structure to be protected are separated by an object called vibration isolator. Incoming mechanical waves are directed back to the source by the isolator, hence target end is protected from exposure to excessive oscillations. Traditionally, vibration isolators are constructed with employing springs and dampers [12,13]. On the other hand, as an innovative approach, periodic structures can be utilized as passive vibration isolators, as well [14-18]. These periodic structures can be Bragg [19,20], local resonance [21,22], or inertial amplification [23,24] types.

In the literature, by employing inertial amplification type periodic structures, one can obtain high performance vibration isolators, in which satisfactory levels of isolation can be achieved for wide frequency ranges. Acar and Yilmaz [25] designed a two-dimensional periodic structure via compliant inertial amplification mechanisms of rectangular type. On that structure, size optimization was performed to enhance vibration stop band properties in the low frequency region. Taniker and Yilmaz [26] investigated a three-dimensional periodic structure constructed with lumped parameter inertial amplification mechanisms in face centered cubic and body centered cubic formations for the purpose of mitigating incoming mechanical vibrations for the low frequency band. Yuksel and Yilmaz [27] designed a two-dimensional periodic structure via shape optimized compliant inertial amplification mechanisms to achieve low frequency vibration isolation. On that study, superiority of shape optimization over size optimization on vibration stop band characteristics was also demonstrated. Taniker and Yilmaz [28] designed a three-dimensional octahedron type periodic structure with triangular type compliant inertial amplification mechanisms for the purpose of achieving three-dimensional vibration isolation for the low frequency region. Frandsen et al. [29] connected periodic lumped parameter inertial amplification mechanisms to a continuous beam structure for the purpose of attaining vibration isolation for a certain frequency band. Taniker and Yilmaz [30] designed a one-dimensional periodic structure via compliant inertial amplification mechanisms with flexure hinges to obtain an ultrawide vibration stop band for the mechanical waves coming from one direction. Yuksel and Yilmaz [31] compared size and topology optimized compliant inertial amplification mechanisms with the same mass regarding to their vibration stop band characteristics. As one suggests, topology optimized periodic structure provided better vibration isolation for a wider frequency range. Barys et al. [32] composed periodic structures with lumped parameter inertial amplification mechanisms and local resonators and they compared these structures with each other. Besides, efficacy of inertial amplification method over local resonance method was investigated and discussed. Orta and Yilmaz [33] designed a one-dimensional periodic low frequency vibration isolator by utilizing compliant inertial amplification mechanisms which converts axial motion to rotary motion. Li et al. [34], formed a periodic structure with composite sandwich beams, which has a lattice structure constructed with both translational and rotational springs inside and lumped inertial amplification mechanisms outside. Yuksel and Yilmaz [35] designed a two-dimensional ultrawide low frequency periodic vibration isolator with topologically optimized compliant inertial amplification mechanisms with flexure hinge connections and instant center of rotation. The proposed design provided ultrawide vibration isolation for the low frequency band, for longitudinal and transverse incoming mechanical waves. Muhammad et al. [36] studied a one-dimensional periodic beam with variable cross-sectional area and attached lumped parameter inertial amplification mechanisms, in order to mitigate transverse mechanical vibration propagation along the structure for a certain frequency range. Yuksel and Yilmaz [37] designed a two-dimensional broadband periodic structure as a vibration isolator with topologically optimized triangular type

basic compliant inertial amplification mechanisms. Mizukami et al. [38] designed a two-dimensional periodic vibration isolator utilizing truss type compliant inertial amplification mechanisms with carbon-fiber composite material. Xi et al. [39], improved a corrugated-core sandwich panel structure's vibration properties by using periodically attached lumped parameter inertial amplification mechanisms with four bar connections. Mi and Yu [40], added periodic lumped parameter inertial amplification mechanisms to the host structure in order to enhance sound transmission of a beam. Miniaci et al. [41], discussed the effect of prestress conditions on vibration isolation stop band properties of a periodic structure constructed with rectangular type compliant inertial amplification mechanisms. Banerjee et al. [42] investigated a lumped parameter periodic structure's vibration isolation band gap properties. The periodic structure was composed of periodic inclusion of lumped inertial amplification mechanisms coupled with local resonators. Li and Zhou [43] formed a periodic structure by using scissor-like inertial amplification mechanisms to reduce low frequency vibration transmission. Er et al. [44], conducted a parametric study on basic rhombus type compliant inertial amplification mechanism configurations to enhance periodic structure's vibration isolation performance. Zeng et al. [45] formed a periodic structure using a distributed parameter inertial amplification model with levered mass configuration. Li et al. [46], examined a periodic structure constructed with lumped parameter elastic inertial amplification mechanism building blocks. Li et al. [47] analyzed a periodic structure, which set up by utilizing a nonlinear lumped parameter inertial amplification mechanism model. Li et al. [48] improved a double beam structure's vibration characteristic via periodically employing double inertial amplification mechanisms throughout the body. Ni and Shi [49] proposed a beam structure with periodically attached levered mass type lumped parameter inertial amplifiers and they studied vibration transmission properties of the suggested frame. As can be seen from the literature review, there are numerous designs that consider vibration isolation properties primarily. However, it is also important for the structure to withstand static loads, as well. To that end, stiffness based optimized isolator designs should also be addressed.

In this study, a one-dimensional periodic vibration isolator is designed using compliant inertial amplification mechanisms as unit cells. In order to maximize the structure's stiffness and reduce the material amount used, topology optimization is conducted on the compliant mechanism. The vibration isolation performance of the topologically stiffness maximized lightweight periodic structure is demonstrated via transmissibility plots.

2. Inertial Amplification Method

Inertial amplification [23, 24] is one of the stop band generation methods available in the literature [50]. A stop band is described as a frequency range (band) in which waves cannot propagate [51]. Hence, a structure with a stop band can be considered to be used as a vibration isolator for the stop band frequency range. Inertial amplification is a powerful stop band creation method, so that, one can obtain vibration isolation frequency bands at low frequency regions without decreasing stiffness or increasing mass of an isolator structure.

2.1. Lumped parameter model

In Figure 1, a lumped parameter inertial amplification mechanism model [25,27] is shown. In this mechanism, masses at two ends (donated with m) are connected with a spring with stiffness k, whereas amplifier mass m_a is connected both of the masses m with rigid links. Rigid links and spring do not possess any mass. At the same time, all masses do not deform, that is to say, they do not have any stiffness value. Hence, the mechanism shown in Figure 1 indicates a discrete (lumped parameter) model. The acute angle between the rigid links and the spring is called as θ. The input vibration y is given from the left side and the output vibration x is received from the right side of the mechanism. Therefore, for small y, and x values, the horizontal displacement of amplifier mass m_a becomes $(x+y)/2$ whereas, the vertical displacement is $(y-x)\cot(\theta)/2$ [52].

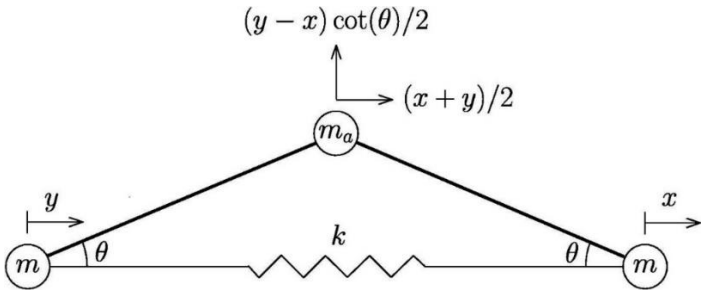

Figure 1. Lumped parameter inertial amplification mechanism.

The equation of motion of the lumped parameter model provided in Figure 1 can be obtained by employing the Lagrange method. For this purpose, the kinetic (T) and the potential (V) energies of the system need to be defined:

$$T = \frac{1}{2}m_a\left[\left(\frac{\dot{x}+\dot{y}}{2}\right)^2 + \left(\frac{\dot{y}-\dot{x}}{2}\cot\theta\right)^2\right] + \frac{1}{2}m\dot{x}^2 + \frac{1}{2}m\dot{y}^2 \quad (1)$$

$$V = \frac{1}{2}k(x-y)^2 \quad (2)$$

Moreover, the Lagrange function ($\mathscr{L}$) is defined as:

$$\mathcal{L} = T - V \quad (3)$$

Hence, the Lagrange function of the system shown in Figure 1 becomes:

$$\mathcal{L} = \frac{1}{2}m_a\left[\left(\frac{\dot{x}+\dot{y}}{2}\right)^2 + \left(\frac{\dot{y}-\dot{x}}{2}\cot\theta\right)^2\right] + \frac{1}{2}m\dot{x}^2 + \frac{1}{2}m\dot{y}^2 \quad -\frac{1}{2}k(x-y)^2 \quad (4)$$

Besides, the Lagrange equation for the generalized coordinate x is given as:

$$\frac{d}{dt}\left(\frac{\partial\mathcal{L}}{\partial\dot{x}}\right) - \frac{\partial\mathcal{L}}{\partial x} = 0 \quad (5)$$

Finally, when Equation (5) is solved for Equation (4), the equation of motion is obtained:

$$[m_a(\cot^2\theta+1)/4 + m]\ddot{x} + kx = [m_a(\cot^2\theta-1)/4]\ddot{y} + ky \quad (6)$$

When the right side of Equation (6) is equated to zero and the left side is solved for the output x, one can obtain the resonance frequency (ω_p) as:

$$\omega_p = \sqrt{\frac{k}{m_a(\cot^2\theta+1)/4+m}} \quad (7)$$

As can be seen from Equation (7), the stiffness value of the system remains as k. On the other hand, by using displacement amplification mechanism, the single degree of freedom system's dynamic mass is increased by $m_a(\cot^2\theta+1)/4$ amount compared to the ordinary mass-spring system's mass m.

Besides, when the left side of Equation (6) is equated to zero and the right side is solved for the input y, one can obtain the antiresonance frequency (ω_z) as:

$$\omega_z = \sqrt{\frac{k}{m_a(\cot^2\theta-1)/4}} \quad (8)$$

As seen from Equations (7) and (8), mechanism's resonance frequency (ω_p) is always lower than its antiresonance frequency (ω_z), which implies that the lumped parameter model in Figure 1 is a vibration isolator of low pass filter type [8]. Vibration transmissibility of this type of isolator can be calculated as a

function of a given excitation frequency by using input and output displacements (respectively y and x) or input and output accelerations (respectively $\ddot{y}$ and $\ddot{x}$) as [25, 27]:

$$TR(\omega_e) = \frac{|x(\omega_e)|}{|y(\omega_e)|} = \frac{|\ddot{x}(\omega_e)|}{|\ddot{y}(\omega_e)|} = \frac{|1-(\omega_e/\omega_z)^2|}{|1-(\omega_e/\omega_p)^2|} \tag{9}$$

where ω_e denotes excitation frequency. When transmissibility value for a given excitation frequency (ω_e) is lower than 1, it means less amount of input oscillations sent from one end can arrive to the output end. Vibration isolation frequency band starts at the frequency limit where the vibration transmissibility value is equal to 1 [25, 27]:

$$\omega_s = \sqrt{\frac{2\omega_p^2\omega_z^2}{\omega_p^2+\omega_z^2}} \tag{10}$$

For the frequencies, which are higher than the stop band starting frequency ω_s, vibration transmissibility value is always lower than 1, hence vibration isolation is achieved. The lumped parameter system in Figure 1 has only one resonance and one antiresonance frequencies. Therefore, vibration stop band created via this mechanism does not have any upper bound (i.e., semi-infinite stop band).

2.2. Compliant inertial amplification mechanism

In Figure 2, a compliant inertial amplification mechanism [25,27] is presented. In compliant mechanisms, bearings and hinges are not utilized. Instead, relative motion between the links are achieved as a result of deflecting flexible members [53]. The compliant inertial amplification mechanism shown in Figure 2 is a distributed parameter system. Hence, it has multiple resonance and antiresonance frequencies, which imply that vibration isolation stop band has an upper bound. It has shown in the literature that, inertial amplification induced vibration stop bands can be created between the first and the second non rigid in plane vibration modes of the compliant mechanism [25,27]. In Figure 2; l_1, l_2, l_3, l_4 denote the lengths and t_1, t_2, t_3, t_4 denote the thicknesses of the corresponding beams.

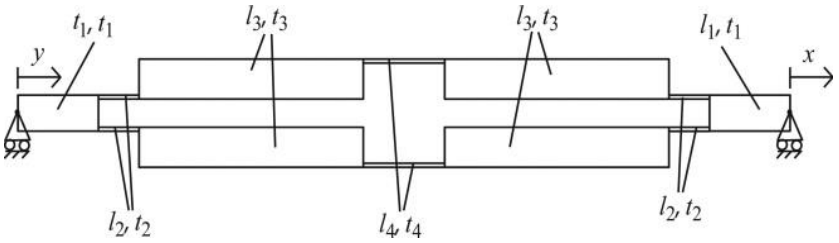

Figure 2. Compliant inertial amplification mechanism.

In order to perform structural topology optimization on this compliant mechanism, finite element method needs to be employed. For this purpose, two-dimensional four node eight degrees of freedom square plane stress finite elements are utilized.

3. Topology Optimization

3.1. General stiffness maximization problem

Topology optimization is the most comprehensive form of structural optimization field since it involves both size and shape optimization while altering a structure's topology [54]. For stiffness maximization (i.e., compliance minimization) topology optimization problems, for a prescribed loading and boundary

conditions, the aim is to find the stiffest structure with certain amount of material. The mathematical description for this kind of optimization problem can be formulated as [55]:

$$\begin{aligned} &\text{minimize}_{\ \boldsymbol{d}}: \quad comp(\boldsymbol{d}) = \boldsymbol{u}^T \boldsymbol{K} \boldsymbol{u} \\ &\text{subject to} \quad : \quad \boldsymbol{K}\boldsymbol{u} = \boldsymbol{f} \\ &\qquad\qquad\quad V(\boldsymbol{d}) = aV_0 \\ &\qquad\qquad\quad \mathbf{0} \le \boldsymbol{d} \le \mathbf{1} \end{aligned} \tag{11}$$

where; $\boldsymbol{u}$ is the global displacement vector, $\boldsymbol{K}$ is the global stiffness matrix, $\boldsymbol{f}$ is the global force vector, V_0 is the design domain volume, $V(\boldsymbol{d})$ is the material volume, a is the volume fraction, $\boldsymbol{d}$ is the design variable vector. Each finite element constituting the design space has an individual design variable value between 0 (void) and 1 (solid). At the end of the optimization process, the aim is to reach a solid or void type of design.

3.2. Topology optimized compliant inertial amplification mechanism

In the literature it has shown both numerically and experimentally that, various versions of structurally optimized compliant inertial amplification mechanism given in Figure 2 isolate incoming excitations effectively for wide frequency bands [25,27,31]. In these optimization studies, vibration isolation frequency band is increased for a given amount of material, hence for the same mass, vibration isolation is achieved for wider frequency regions. On the other hand, for some circumstances, it could be desirable for a vibration isolator to be able to carry load. Therefore, stiffness of a vibration isolator should also be taken into account in the design process, as well. So far, the effort shown concentrated on increasing the stop band frequency range. Yet, in this study, another important design criterion, stiffness is considered. In order to observe the relationship between the stiffness and vibration isolation performance of the compliant mechanism provided in Figure 2, topology optimization studies are conducted.

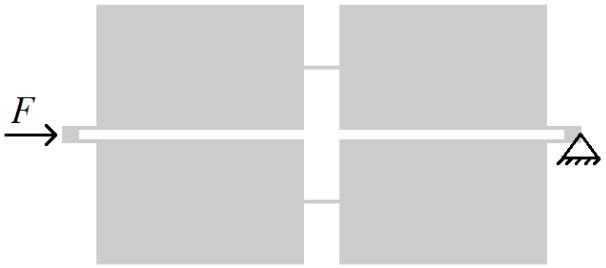

Figure 3. Stiffness maximization (compliance minimization) topology optimization problem design space.

In Figure 3, stiffness maximization topology optimization problem design space is shown. A unit static force is applied on the left side of the mechanism while at the right end pinned boundary condition is employed. Since, a one-dimensional periodic structure will be formed via incorporating the mechanism in horizontal alignment, stiffness maximization for this direction is considered. The mechanism has 120 mm length in horizontal and 60 mm width in vertical dimensions. The finite element discretization of the design space is 120 × 60. That is to say, 7200 four node eight degrees of freedom plane stress elements with 1 mm × 1 mm dimensions are utilized. Besides, beam dimensions are determined as: l_1=4 mm, t_1 = 4 mm, l_2 = 4 mm, t_2 = 1 mm, l_3 = 48 mm, t_3 = 29 mm, l_4 = 8 mm, t_4 = 1 mm. Moreover, the 4th beams connect to the 3rd beams at the middle. An isotropic material with modulus of elasticity E=210 GPa, Poisson's ratio ν = 0.3 and density ρ = 7800 kg/m^3 is considered.

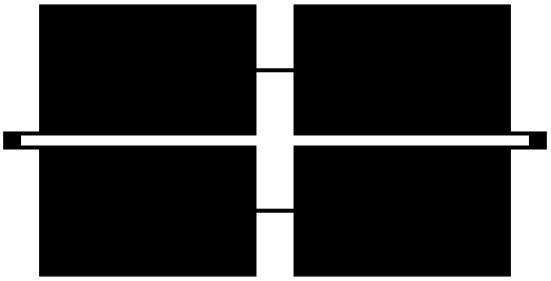

Figure 4. Compliant inertial amplification mechanism design with 100 % material utilized.

In topology optimization, an open source MATLAB code [55] and a post-processing filter [56] are utilized, and stiffness maximized inertial amplification mechanisms are obtained for several percent material volume fraction values. In Figure 4, a design, which has 100 % material utilized, is shown. As can be seen, it is a design in which the design space in Figure 3 is fully solid. For other material volume fraction values, the optimization problem presented in Eq. (11) is solved. In Figure 5, several stiffness maximized designs are shown, for which, 100 %, 80 %, 60 % and 40 % material in the design space is utilized. Figure 5, also shows the evolutionary path of the stiffness maximized mechanism as a function of material percentage utilized. It is important to note that, optimized structures' stiffness values almost remain the same. For instance, the difference between the stiffness values of the mechanism with 100 % material utilized (Figure 5a) and the mechanism with 40 % material utilized (Figure 5d) is only 0.06 %, which implies that the stiffness values are essentially the same. Such a result is expected, since the axial stiffness of the mechanism primarily depends on the dimensions of the flexure hinges (i.e., beams enumarated as 2 and 4) and their connection positions to the remaining parts (i.e., beams enumarated as 1 and 3) [31,35].

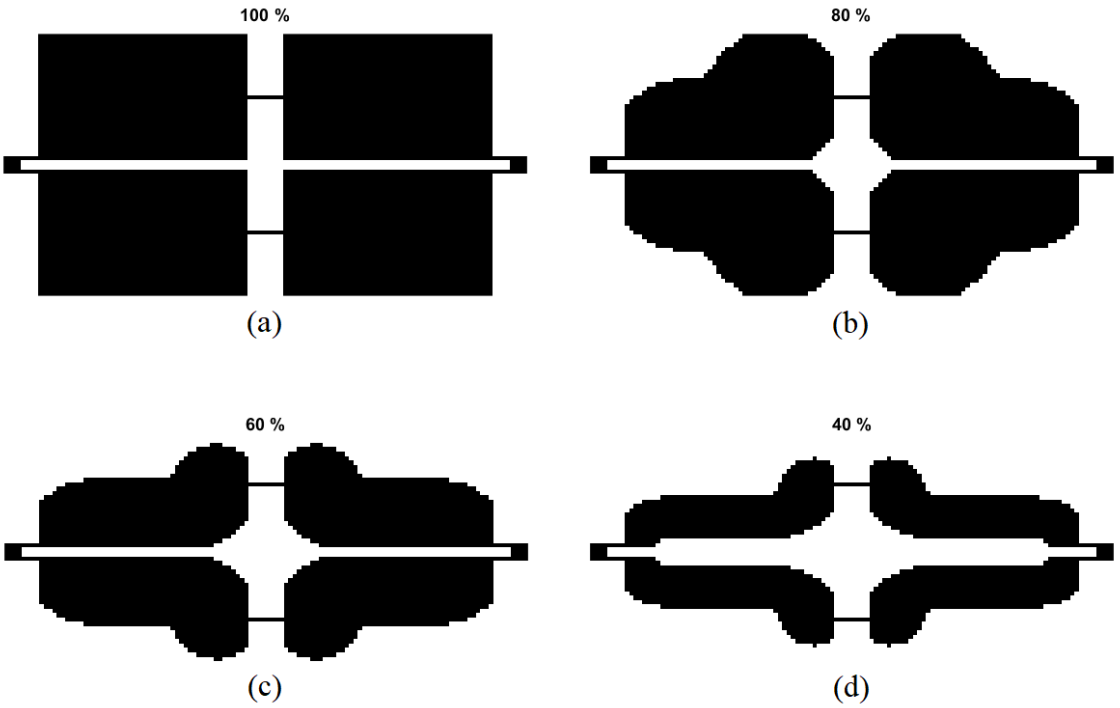

Figure 5. Designs with various material percentages utilized in the design space: (a) design with 100 % material used, (b) design with 80 % material used, (c) design with 60 % material used, (d) design with 40 % material used. To note that, stiffness values for all of the mechanisms from (a) to (d) are essentially the same (e.g., the difference between the stiffness values for 100 % material utilized design and 40 % material utilized design is only 0.06 %.)

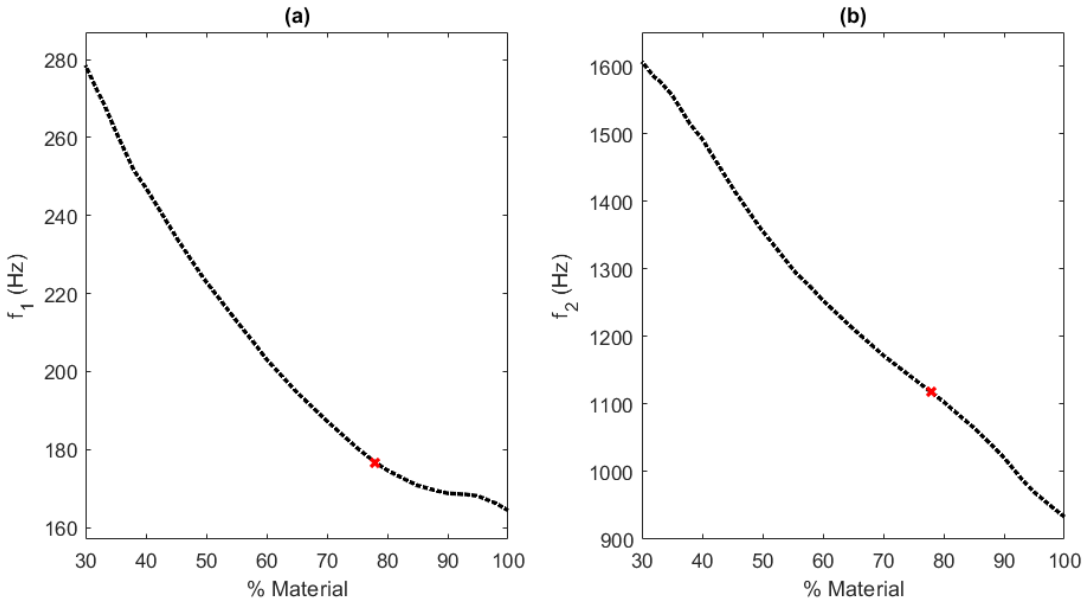

Figure 6. Variation of (a) first and (b) second natural frequencies of distributed parameter inertial amplification mechanism model with respect to % material (volume fraction) of the design space given in Fig. 3. Red cross indicates the values for the topology optimized design in Fig. 8 and 100 % indicates the values for the design in Fig. 4.

As stiffness of the structure given in Figure 3 essentially remains the same independent of the material amount used, an optimization process's rational aim becomes to achieve the widest vibration stop band possible with the least amount of material utilized. To that end, vibration isolation performance of several stiffness maximized compliant mechanisms are compared for material volume fraction values of 30 % to 100 %. As the stop band occurs between the first and the second non rigid in-plane modes of the compliant mechanism [25, 27,31], the lower and the upper limits of vibration isolation frequency region are dictated by these two frequencies. As a result, in Figure 6 in order to compare stop band widths, the first and the second non rigid in-plane mode frequency values are tabulated. Moreover, to analyze the stop band width more clearly, the ratio of these two mode frequencies (i.e., f_2/f_1) are calculated in the literature frequently [25,27,31,57]. In Figure 7, the variation of f_2/f_1 ratio with respect to percent material utilized is shown. As can be seen, the maximum stop band width is achieved for 78% material volume fraction value with f_2/f_1 ratio value of 6.32. Whereas, for the original mechanism shown in Figure 4 with 100 % material volume fraction value, f_2/f_1 ratio value is found as 5.68. Therefore, as a result of topology optimization, vibration isolation stop band width can be increased by 11 % by using 22 % less material in the compliant mechanism. The topology optimized compliant inertial amplification mechanism design with 78 % material volume fraction value is presented in Figure 8.

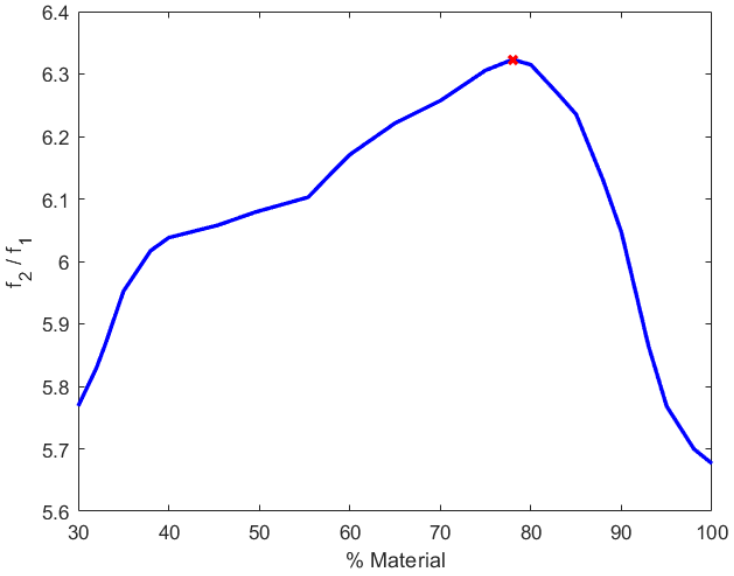

Figure 7. Variation of f_2/f_1 ratio with respect to % material (volume fraction). Red cross indicates the values for the design in Figure 8 and 100 % indicates the values for the design in Figure 4.

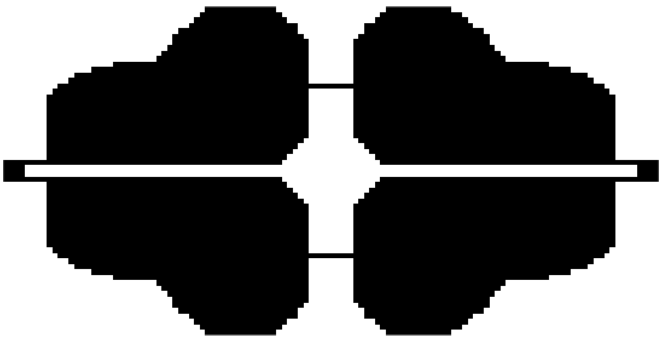

Figure 8. Topology optimized inertial amplification mechanism, i.e., the design with 78 % material used.

4. Numerical Results

In this section, vibration isolation performance of unit cell and periodic structures are demonstrated via transmissibility plots and compared.

4.1. Unit cell mechanisms

A unit cell is the smallest repeating unit of a periodic structure. The first unit cell considered is the compliant inertial amplification mechanism design with 100 % material utilized (see Figure 4). The second unit cell is the topology optimized inertial amplification mechanism with 78 % material used (see Figure 8). The first two non rigid mode shapes of these two unit cell mechanisms are provided in Figure 9. Both mechanisms perform similar mode shape motions for their first two modes, which is a result that is in accordance with the literature [25,27,31]. Note that, for both of the unit cells, vibration isolation stop band starts just above the first natural frequency and ends just below the second natural frequency, which can be regarded (with small error introduced) as the stop band limits are f_1 and f_2 [25,27,31]. As the stiffness value remains essentially the same, the first modes appear almost for the same frequency values. The small discrepancy stems from the fact that topology optimized design has less weight, which shifts the first natural frequency of the topology optimized

design by a factor of $1/\sqrt{m}$, a result which can be observed in nonlinear behavior seen in Figure 6(a). On the other hand, as a result of topology optimization, second natural frequency is shifted away for the topology optimized design compared to the original compliant mechanism.

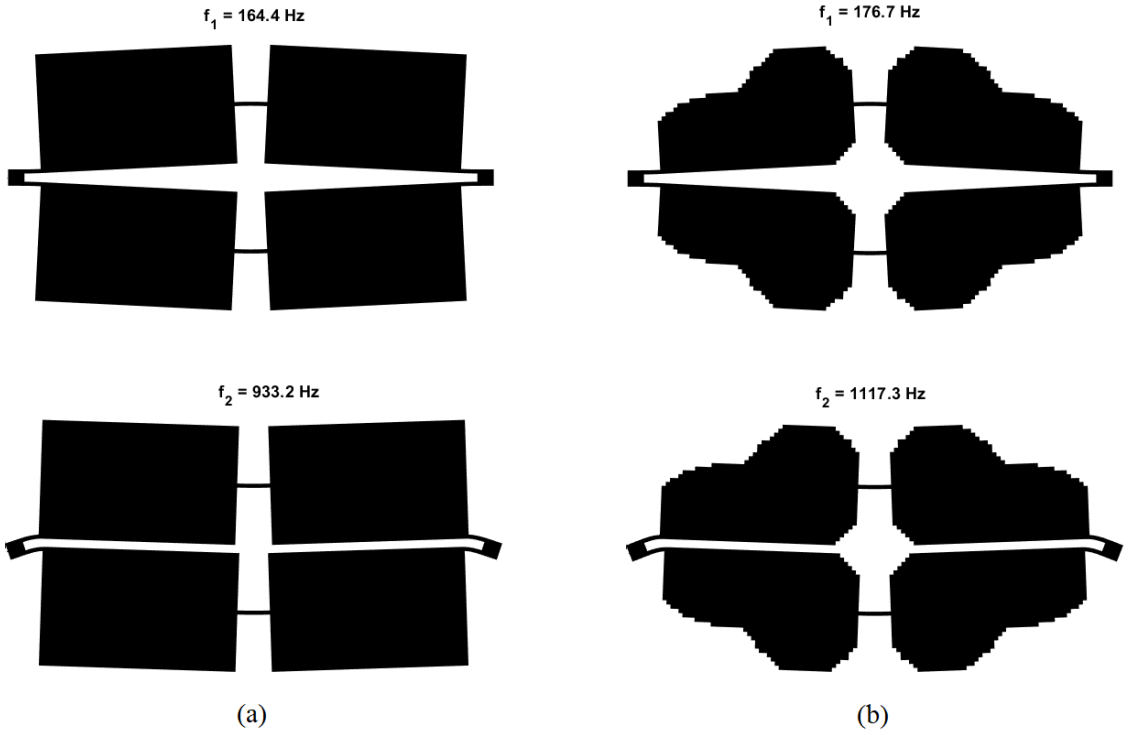

Figure 9. The first two mode shapes of distributed parameter inertial amplification mechanisms. (a) Compliant mechanism. (b) Topology optimized mechanism.

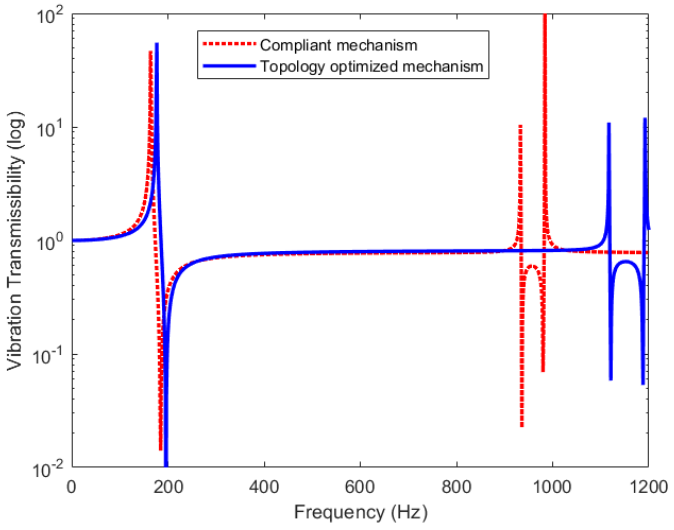

Figure 10. Vibration transmissibility comparison of unit cell compliant (red dotted line) and topology optimized (blue solid line) inertial amplification mechanisms.

In order to compare the vibration isolation performances of the original (Figure 4) and the topology optimized (Figure 8) unit cell designs, vibration transmissibility plots for these two mechanisms are provided in Figure 10. As can be seen, for both of the designs, similar vibration isolation levels (around 20 %) are achieved for most of the stop band. On the other hand, topology optimized design provides wider vibration stop band compared to the original compliant mechanism. For the original compliant mechanism in Figure 4 vibration isolation is achieved between 174 Hz – 926 Hz, whereas for the topology optimized compliant mechanism in Figure 8 vibration isolation is obtained between 186 Hz – 1106 Hz. Therefore, by utilizing 22

% less construction material, topology optimized design provides vibration isolation for wider frequency band as compared to the original mechanism.

4.2. Periodic structures

In order to achieve high performance vibration isolation, compliant mechanisms demonstrated in Figure 4 and Figure 8 can be used as unit cells to form periodic structures. It has been shown in the literature that, vibration isolation starting and ending frequencies will be approximately the same as the unit cell mechanisms', whereas vibration isolation levels rise as the number of unit cells (compliant mechanisms) utilized in the periodic structures is increased [25, 27, 31, 35]. In Figure 11, a sample periodic structure, which is formed via incorporating 3 original compliant inertial amplification mechanisms in a one-dimensional array, is shown. Input excitation (y) is provided to this periodic structure from one end and output response (x) is taken from the other end. Then, vibration transmissibility is calculated with finite element method. The vibration transmissibility of the periodic structure in Figure 11 is demonstrated in Figure 12 as red dashed line. As can be seen, between 168 Hz – 931 Hz, vibration isolation is achieved. Moreover, in Figure 12, the effect of employing more mechanisms (unit cells) in the formation of periodic structures are clearly seen. As the number of, unit cells utilized increases, vibration isolation levels increase, as well. For instance, the periodic structure formed via incorporating 8 original compliant inertial amplification mechanisms provide 99.9 % vibration isolation for almost entire of the stop band frequency range between 165 Hz – 933 Hz (blue solid line in Figure 12). Please note that, as the number of unit cell mechanisms utilized in the periodic structure increase, stop band starting and ending frequencies closely resemble the first and the second natural frequencies of the unit cell (i.e., f_1 = 164.4 Hz, f_2 = 933.2 Hz; also see Figure 9a).

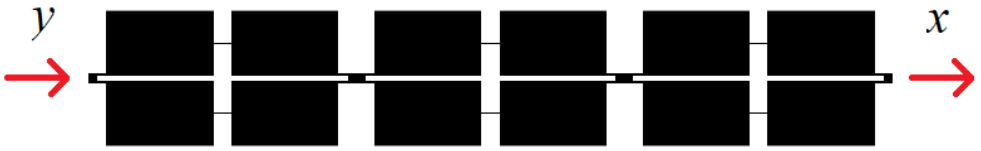

Figure 11. Sample periodic structure constructed with 3 compliant unit cell mechanisms given in Figure 4.

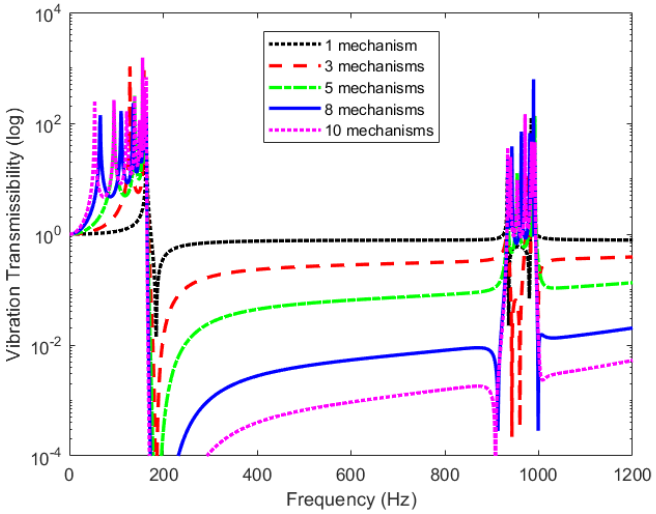

Figure 12. Vibration transmissibility plots of periodic structures formed with various number of compliant unit cell mechanisms shown in Figure 4.

With the same methodology, periodic structures by utilizing various number of topology optimized unit cell mechanisms in Figure 8 can be constructed, as well. A sample one-dimensional periodic structure, formed via incorporating 3 topology optimized inertial amplification mechanisms, is shown in Figure 13. As for the

previous case, input excitation (y) is provided from one end and output response (x) is taken from the other end. Consequently, vibration transmissibility is calculated (the red dashed line in Figure 14). Vibration transmissibilities of periodic structures, formed using several topology optimized inertial amplification mechanisms as unit cells, are shown in Figure 14. As can be seen, for all of the periodic structures, vibration isolation frequency range (stop band) closely resembles the first and the second natural frequencies of the topology optimized design (see Figure 9b). On the other hand, as the number of unit cell mechanisms utilized in the periodic structure increase, vibration isolation levels increase, as well. For example, for almost all of the frequency range between 178 Hz – 1117 Hz, 99 % vibration isolation is achieved by the periodic structure formed via incorporation of 8 topology optimized compliant inertial amplification mechanisms (see the blue solid line in Figure 14).

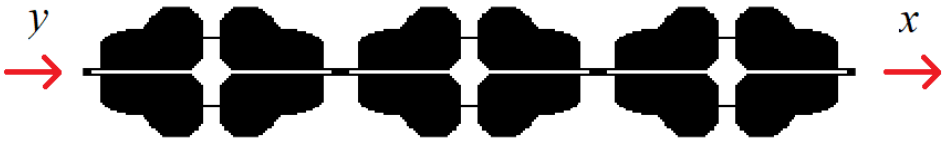

Figure 13. Sample periodic structure constructed with 3 topology optimized unit cell mechanisms given in Figure 8.

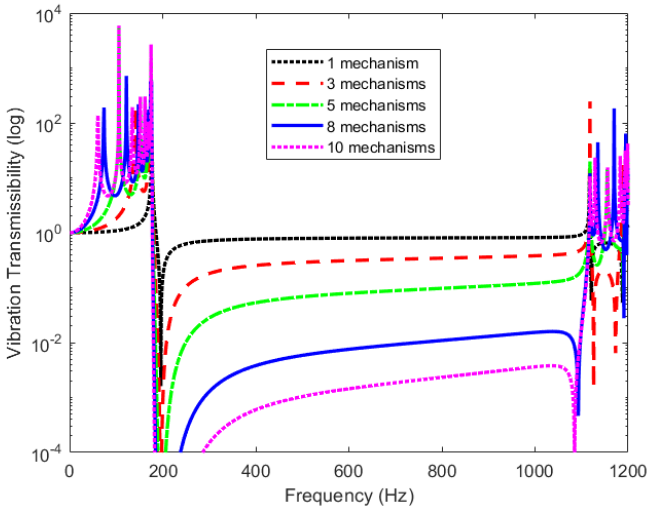

Figure 14. Vibration transmissibility plots of periodic structures formed with various number of topology optimized unit cell mechanisms shown in Figure 8.

As can be observed from Figures 12 and 14, periodic structures formed with topology optimized inertial amplification mechanisms provide satisfactory vibration isolation for wider frequency range with utilizing less construction material but having the same axial stiffness value of the original mechanism. In order to make the comparison more comprehensive, vibration transmissibility plots of two periodic structures formed with utilizing 8 original and 8 topology optimized mechanisms is shown in Figure 15. As can be seen, topology optimized periodic structure provides vibration isolation for 11 % wider frequency range by using 22 % less material. On the other hand, the vibration isolation levels of topology optimized periodic structure is slightly less than the original periodic structure, i.e., 99 % vs 99.9 %, which is a difference that can be neglected for practical purposes. Moreover, as the axial stiffness values of the unit cell mechanisms are almost the same, both periodic structures can withstand the same loading conditions.

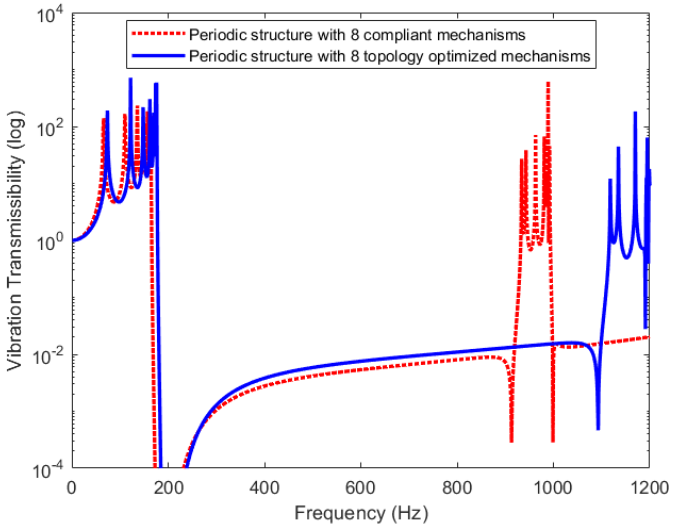

Figure 15. Vibration transmissibility comparison of periodic structures formed with 8 compliant (red dotted line) and 8 topology optimized (blue solid line) inertial amplification mechanisms.

4.3. Comparison of the results with the literature

Although the compliant inertial amplification mechanism topology represented in Fig. 2 has been studied before [25,27,28,31,37,58], there is not a study conducted on design of such mechanisms considering stiffness properties as its main objective function yet. Therefore, this work's major contribution to the literature is obtaining a topologically optimized complaint inertial amplification mechanism with maximized stiffness value. However, a comparison of the results of the current study and the existing ones [27,58] which considers stiffness as a constraint in their optimization problem formulation can be insightful, as well.

In Yuksel and Yilmaz [27], size optimized and shape optimized mechanisms were designed with each has a stiffness value of 1000 kN/m. The material selected was steel with modulus of elasticity value of 205 GPa, Poisson's ratio value of 0.29 and density value of 7800 kg/m^3. Using shell elements in the finite element analysis, shape optimized design's f_2/f_1 ratio was calculated as 3.13 whereas, size optimized design has a 2.63 f_2/f_1 ratio value. Moreover, two dimensional structural area of the designs were each 896 mm^2. Again, in Yuksel and Yilmaz [58], size optimized and shape optimized mechanisms were obtained with each has a stiffness value of 1000 kN/m. The material selected was steel with modulus of elasticity value of 210 GPa, Poisson's ratio value of 0.29 and density value of 7800 kg/m^3. Using one dimensional beam elements with eccentricity in the finite element analysis, shape optimized design's f_2/f_1 ratio was calculated as 3.34 whereas, size optimized design has a 2.82 f_2/f_1 ratio value. Besides, two dimensional structural area of the designs were each 961 mm^2. As a result, the values obtained for these two studies can be considered as almost identical ignoring the finite element type utilized and small differences in material area. It should be noted that, in the studies mentioned in Yuksel and Yilmaz [27] and [58], the objective function was to maximize the ratio of f_2/f_1, whereas stiffness is given as a constraint of both size and shape optimization problems.

On the other hand, in this study, final topologically optimized design has a stiffness value of 55500 kN/m which is much higher compared to the designs provided in Yuksel and Yilmaz [27] and [58]. Although the material properties are similar, the discrepancy stems from thick compliant hinge connections (i.e., 2nd and 4th beams) and the objective function of the topology optimization problem which is stiffness maximization. Moreover, material area of the current design is 3488 mm^2, which is much larger than the structures' indicated in Yuksel and Yilmaz [27] and [58]. As a result, a higher value of 6.32 for f_2/f_1 ratio is achieved. In summary, a much stiff structure with a broad vibration isolation frequency band is attained with a cost of increased material area compared to the investigated studies [27,58] that are found in the literature.

Moreover, as a final comparison with the work of Yuksel and Yilmaz [31] can be done to investigate the differences between the topologically optimized designs obtained with employment of different objective functions. In Yuksel and Yilmaz [31], the topology optimization problem's objective function was the maximization of the f_2/f_1 ratio of the unit cell mechanism. Although the material of construction was steel with the same modulus of elasticity and Poisson's ratio values used in this study, the design space was 100 mm by 50 mm, which is significantly smaller than the current study. Since the primary concern was achieving the highest frequency gap (i.e., vibration stop band) available, f_2/f_1 ratio was obtained as 6.07 as a result of solution of the dynamic topology optimization problem. f_1 is achieved at 304.4 Hz whereas f_2 is achieved at 1847.7 Hz. Material area of the topologically optimized design obtained in Yuksel and Yilmaz [31] is 1512 mm^2 which is 56.7 % less than the current design obtained in this study. The discrepancy between the results obtained from Yuksel and Yilmaz [31] and the current study stems from the fact that, the current study's design has much more weight, hence its first natural frequency occurs at 176.7 Hz, which is 41.6 % below than the design in Yuksel and Yilmaz [31]. In addition to the increase in the weight, the current design is longer and wider, hence the resulting second frequency is 39.5 % lower than the design in Yuksel and Yilmaz [31]. That, difference makes f_2/f_1 ratio of the design provided in Yuksel and Yilmaz [31] as 3.96 % less than the current design presented in this study. Moreover, the stiffness value for the design given in Yuksel and Yilmaz [31] is calculated as 41400 kN/m, which is 25.4 % less than the current design. To sum up, the topologically optimized mechanism in Yuksel and Yilmaz [31] provides a vibration isolation for a fairly large frequency range with much less amount of material, which is a result coincides with the objective function of that study, which is frequency gap maximization. On the other hand, in the current study, the objective function is to attain the stiffest possible structure, hence a stiffer structure which has approximately the same frequency range of vibration is achieved at the expense of increasing the optimized mechanism's weight.

4. Conclusion

In this study, a lightweight periodic structure, which can be used as a high-performance vibration isolator, is considered. A compliant mechanism's weight is reduced via topology optimization while stiffness of the structure is maintained. Among available topology optimized mechanisms, a design which provides vibration isolation for the widest frequency range possible, is chosen. The selected design has 22 % less weight and provides vibration isolation for a frequency range which is 11 % higher than the original mechanism. By using the topology optimized mechanisms, sample periodic structures are formed and vibration transmissibility plots indicate that high vibration isolation levels can be achieved. It is shown that, a periodic structure formed with 8 topology optimized mechanisms provide 99 % vibration isolation for almost all of the frequency range between 178 Hz – 1117 Hz.

Conflict of Interest Statement

The authors declare that there is no conflict of interest

References

[1] S. Daley, F. A. Johnson, J. B. Pearson and R. Dixon, "Active vibration control for marine applications," *Control Engineering Practice*, vol. 12, no. 4, pp. 465-474, 2004. doi:10.1016/S0967-0661(03)00135-7

[2] Y. H. Guan, T. C. Lim and W. S. Shepard, "Experimental study on active vibration control of a gearbox system," *Journal of Sound and Vibration*, vol. 282, no. 3-5, pp. 713-733, 2005. doi:10.1016/j.jsv.2004.03.043

[3] S. M. Kuo, S. Mitra and W. S. Gan, "Active noise control system for headphone applications," *IEEE Transactions on Control Systems Technology*, vol. 14, no. 2, pp. 331-335, 2006. doi:10.1109/TCST.2005.863667

[4] S. M. Khot, P. Y. Nitesh, R. Tomar, S. Desai and S. Vittal, "Active vibration control of cantilever beam by using PID based output feedback controller," *Journal of Vibration and Control,* vol. 18, no. 3, pp. 366-372, 2012. doi:10.1177/1077546311406307

[5] O. Yuksel and C. Yilmaz, "Active noise control in a duct with flow," *Journal of Dynamic Systems, Measurement and Control,* vol. 136, no. 3, p. 031014, 2014. doi:10.1115/1.4026410

[6] A. Zippo, G. Ferrari, M. Amabili, M. Barbieri and F. Pellicano, "Active vibration control of a composite sandwich plate," *Composite Structures,* vol. 128, pp. 100-114, 2015. doi:10.1016/j.compstruct.2015.03.037

[7] M. Moshrefi-Torbati, A. J. Keane, S. J. Elliott, M. J. Brennan and E. Rogers, "Passive vibration control of a satellite boom structure by geometric optimization using genetic algorithm," *Journal of Sound and Vibration,* vol. 267, no. 4, pp. 879-892, 2003. doi:10.1016/S0022-460X(03)00192-5

[8] C. Yilmaz and N. Kikuchi, "Analysis and design of passive low-pass filter-type vibration isolators considering stiffness and mass limitations," *Journal of Sound and Vibration,* vol. 293, no. 1-2, pp. 171-195, 2006. doi:10.1016/j.jsv.2005.09.016

[9] D. Kamesh, R. Pandiyan and A. Ghosal, "Passive vibration isolation of reaction wheel disturbances using a low frequency flexible space platform," *Journal of Sound and Vibration,* vol. 331, no. 6, pp. 1310-1330, 2012. doi:10.1016/j.jsv.2011.10.033

[10] E. A. Ribeiro, J. T. Pereira and C. A. Bavastri, "Passive vibration control in rotor dynamics: Optimization of composed support using viscoelastic materials," *Journal of Sound and Vibration,* vol. 351, pp. 43-56, 2015. doi:10.1016/j.jsv.2015.04.007

[11] Z. Wu, X. Jing, B. Sun and F. Li, "A 6DOF passive vibration isolator using X-shape supporting structures," *Journal of Sound and Vibration,* vol. 380, pp. 90-111, 2016. doi:10.1016/j.jsv.2016.06.004

[12] S. S. Rao, "Vibration Control," Mechanical Vibrations. Upper Saddle River: Prentice Hall, 2011.

[13] D. J. Inman, "Design for Vibration Suppression," Engineering Vibration. Upper Saddle River: Pearson Education, 2014.

[14] J. Wen, G. Wang, D. Yu, H. Zhao and Y. Liu, "Theoretical and experimental investigation of flexural wave propagation in straight beams with periodic structures: Application to a vibration isolation structure," *Journal of Applied Physics,* vol. 97, no. 11, p. 114907, 2005. doi:10.1063/1.1922068

[15] G. Wang, X. Wen, J. Wen and Y. Liu, "Quasi-one-dimensional periodic structure with locally resonant band gap," *Journal of Applied Mechanics,* vol. 73, no. 1, pp. 167-170, 2006. doi:10.1115/1.2061947

[16] J. H. Oh, S. Qi, Y. Y. Kim and B. Assouar, "Elastic metamaterial insulator for broadband low-frequency flexural vibration shielding," *Physical Review Applied,* vol. 8, no. 5, p. 054034, 2017. doi:10.1103/PhysRevApplied.8.054034

[17] R. Prasad and A. Sarkar, "Broadband vibration isolation for rods and beams using periodic structure theory," *Journal of Applied Mechanics,* vol. 86, no. 2, p. 021004, 2019. doi:10.1115/1.4042011

[18] L. D'Alessandro, R. Ardito, F. Braghin and A. Corigliano, "Low frequency 3D ultra-wide vibration attenuation via elastic metamaterial," *Scientific Reports,* vol. 9, p. 8039, 2019. doi:10.1038/s41598-019-44507-6

[19] M. Sigalas and E. N. Economou, "Elastic and acoustic wave band structure," *Journal of Sound and Vibration,* vol. 158, no. 2, pp. 377-382, 1992. doi:10.1016/0022-460X(92)90059-7

[20] M. Sigalas and E. N. Economou, "Band structure of elastic waves in two dimensional systems," *Solid State Communications,* vol. 86, no. 3, pp. 141-143, 1993. doi:10.1016/0038-1098(93)90888-T

[21] Z. Liu, X. Zhang, Y. Mao, Y. Y. Zhu, Z. Yang, C. T. Chan and P. Sheng, "Locally resonant sonic materials," Science, vol. 289, no. 5485, pp. 1734-1736, 2000. doi:10.1126/science.289.5485.1734

[22] C. Goffaux and J. Sánchez-Dehesa, "Two-dimensional phononic crystals studied using a variational method: application to lattices of locally resonant materials," *Physical Review B,* vol. 67, no. 14, p. 144301, 2003. doi:10.1103/PhysRevB.67.144301

[23] C. Yilmaz, G. M. Hulbert and N. Kikuchi, "Phononic band gaps induced by inertial amplification in periodic media," *Physical Review B,* vol. 76, no. 5, p. 054309, 2007. doi:10.1103/PhysRevB.76.054309

[24] C. Yilmaz and G. M. Hulbert, "Theory of phononic gaps induced by inertial amplification in finite structures," *Physics Letters A,* vol. 374, no. 34, pp. 3576-3584, 2010. doi:10.1016/j.physleta.2010.07.001

[25] G. Acar and C. Yilmaz, "Experimental and numerical evidence for the existence of wide and deep phononic gaps induced by inertial amplification in two-dimensional solid structures," *Journal of Sound and Vibration*, vol. 332, no. 24, pp. 6389-6404, 2013. doi:10.1016/j.jsv.2013.06.022

[26] S. Taniker and C. Yilmaz, "Phononic gaps induced by inertial amplification in BCC and FCC lattices," *Physics Letters A*, vol. 377, no. 31-33, pp. 1930-1936, 2013. doi:10.1016/j.physleta.2013.05.022

[27] O. Yuksel and C. Yilmaz, "Shape optimization of phononic band gap structures incorporating inertial amplification mechanisms," *Journal of Sound and Vibration*, vol. 355, pp. 232-245, 2015. doi:10.1016/j.jsv.2015.06.016

[28] S. Taniker and C. Yilmaz, "Design, analysis and experimental investigation of three-dimensional structures with inertial amplification induced vibration stop bands," *International Journal of Solids and Structures*, vol. 72, pp. 88-97, 2015. doi:10.1016/j.ijsolstr.2015.07.013

[29] N. M. M. Frandsen, O. R. Bilal, J. S. Jensen and M. I. Hussein, "Inertial amplification of continuous structures: Large band gaps from small masses," *Journal of Applied Physics*, vol. 119, p. 124902, 2016. doi:10.1063/1.4944429

[30] S. Taniker and C. Yilmaz, "Generating ultra wide vibration stop bands by a novel inertial amplification mechanism topology with flexure hinges," *International Journal of Solids and Structures*, vol. 106, pp. 129-138, 2017. doi:10.1016/j.ijsolstr.2016.11.026

[31] O. Yuksel and C. Yilmaz, "Size and topology optimization of inertial amplification induced phononic band gap structures," in *Proceedings of the ASME International Mechanical Engineering Congress and Exposition*, Tampa, Florida, USA, 2017. p. V013T01A007. doi:10.1115/IMECE2017-71342

[32] M. Barys, J. S. Jensen and N. M. M. Frandsen, "Efficient attenuation of beam vibrations by inertial amplification," *European Journal of Mechanics-A/Solids*, vol. 71, pp. 245-257, 2018. doi:10.1016/j.euromechsol.2018.04.001

[33] A. H. Orta and C. Yilmaz, "Inertial amplification induced phononic band gaps generated by a compliant axial to rotary motion conversion mechanism," *Journal of Sound and Vibration*, vol. 439, pp. 329-343, 2019. doi:10.1016/j.jsv.2018.10.014

[34] J. Li, P. Yang and S. Li, "Phononic band gaps by inertial amplification mechanisms in periodic composite sandwich beam with lattice truss cores," *Composite Structures*, vol. 231, p. 111458, 2020. doi:10.1016/j.compstruct.2019.111458

[35] O. Yuksel and C. Yilmaz, "Realization of an ultrawide stop band in a 2-D elastic metamaterial with topologically optimized inertial amplification mechanisms," *International Journal of Solids and Structures*, vol. 203, pp. 138-150, 2020. doi:10.1016/j.ijsolstr.2020.07.018

[36] S. Muhammad, S. Wang, F. Li and C. Zhang, "Bandgap enhancement of periodic nonuniform metamaterial beams with inertial amplification mechanisms," *Journal of Vibration and Control*, vol. 26, no. 15-16, pp. 1309-1318, 2020. doi:10.1177/1077546319895630

[37] O. Yuksel and C. Yilmaz, "Design of a broadband elastic metamaterial via topologically optimized inertial amplification mechanisms," in *Proceedings of the 11th International Conference on Structural Dynamics*, Athens, Greece, 2020. pp. 4125-4138. doi:10.47964/1120.9337.19454

[38] K. Mizukami, K. Funaba and K. Ogi, "Design and three-dimensional printing of carbon-fiber-composite elastic metamaterials with inertial amplification mechanisms," *Journal of Sound and Vibration*, vol. 513, p. 116412, 2021. doi:10.1016/j.jsv.2021.116412

[39] C. Xi, L. Dou, Y. Mi and H. Zheng, "Inertial amplification induced band gaps in corrugated-core sandwich panels," *Composite Structures*, vol. 267, p. 113918, 2021. doi:10.1016/j.compstruct.2021.113918

[40] Y. Mi and X. Yu, "Sound transmission of acoustic metamaterial beams with periodic inertial amplification mechanisms," *Journal of Sound and Vibration*, vol. 499, p. 116009, 2021. doi:10.1016/j.jsv.2021.116009

[41] M. Miniaci, M. Mazzotti, A. Amendola and F. Fraternali, "Effect of prestress on phononic band gaps induced by inertial amplification," *International Journal of Solid and Structures*, vol. 216, pp. 156-166, 2021. doi:10.1016/j.ijsolstr.2020.12.011

[42] A. Banerjee, S. Adhikari and M. I. Hussein, "Inertial amplification band-gap generation by coupling a levered mass with a locally resonant mass," *International Journal of Mechanical Sciences*, vol. 207, p. 106630, 2021. doi:10.1016/j.ijmecsci.2021.106630

[43] Y. Li and W. Zhou, "Bandgap and vibration transfer characteristics of scissor-like periodic metamaterials," *Journal of Applied Physics*, vol. 130, p. 025103, 2021. doi:10.1063/5.0047119

[44] E. Er, E. Türkeş and O. Yüksel, "A parametric investigation on various compliant inertial amplification mechanisms for a periodic vibration isolator design," *Gazi Journal of Engineering Sciences*, vol. 8, no. 3, pp. 511-523, 2022. doi:10.30855/gmbd.0705039

[45] Y. Zeng, L. Cao, S. Wan, T. Guo, Y. F. Wang, Q. J. Du, B. Assouar and Y. S. Wang, "Seismic metamaterials: Generating low-frequency bandgaps induced by inertial amplification," *International Journal of Mechanical Sciences,* vol. 221, p. 107224, 2022. doi:10.1016/j.ijmecsci.2022.107224

[46] Y. Li, N. Zhao and S. Yao, "Theoretical analysis of 2D meta-structure with inertia amplification," *International Journal of Mechanical Sciences,* vol. 235, p. 107717, 2022. doi:10.1016/j.ijmecsci.2022.107717

[47] Y. Li, N. Zhao and S. Yao, "Nonlinear dynamics of 1D meta-structure with inertia amplification," *Applied Mathematical Modelling,* vol. 118, pp. 728-744, 2023. doi:10.1016/j.apm.2023.01.039

[48] H. Li, Y. Li and X. Liu, "Double-beam metastructure with inertially amplified resonators for flexural wave attenuation," *European Journal of Mechanics – A / Solids,* vol. 97, p. 104794, 2023. doi:10.1016/j.euromechsol.2022.104794

[49] A. Ni and Z. Shi, "Inertial amplified topological metamaterial beams," *Journal of Applied Physics,* vol. 133, p. 065105, 2023. doi:10.1063/5.0140790

[50] Y. F. Wang, Y. Z. Wang, B. Wu, W. Chen and Y. S. Wang, "Tunable and active phononic crystals and metamaterials," *Applied Mechanics Reviews,* vol. 72, no. 4, p. 040801, 2020. doi:10.1115/1.4046222

[51] C. Yilmaz and G. M. Hulbert, "Dynamics of Locally Resonant and Inertially Amplified Lattice Materials," Dynamics of Lattice Materials. West Sussex: John Wiley & Sons, 2017.

[52] H. W. Ma, S. M. Yao, L. Q. Wang and Z. Zhong, "Analysis of the displacement amplification ratio of bridge-type flexure hinge," *Sensors and Actuators A: Physical,* vol. 132, no. 2, pp. 730-736, 2006. doi:10.1016/j.sna.2005.12.028

[53] L. L. Howell, "Introduction to Compliant Mechanisms," Handbook of Compliant Mechanisms. West Sussex: John Wiley & Sons, 2013.

[54] O. Yüksel, "An overview on topology optimization methods employed in structural engineering," *Kırklareli University Journal of Engineering and Science,* vol. 5, no. 2, pp. 159-175, 2019. doi:10.34186/klujes.606666

[55] E. Andreassen, A. Clausen, M. Schevenels, B. S. Lazarov and O. Sigmund, "Efficient topology optimization in MATLAB using 88 lines of code," *Structural and Multidisciplinary Optimization,* vol. 43, no. 1, pp. 1-16, 2011. doi:10.1007/s00158-010-0594-7

[56] O. Sigmund and K. Maute, "Topology optimization approaches," *Structural and Multidisciplinary Optimization,* vol. 48, no. 6, pp. 1031-1055, 2013. doi:10.1007/s00158-013-0978-6

[57] J. S. Jensen and N. L. Pedersen, "On maximal eigenfrequency separation in two-material structures: the 1d and 2d scalar cases," *Journal of Sound and Vibration,* vol. 289, no. 4-5, pp. 967-986, 2006. doi:10.1016/j.jsv.2005.03.028

[58] O. Yuksel and C. Yilmaz, "Obtaining inertial amplification induced phononic gaps via structural optimization of a compliant mechanism," in *Proceedings of the 11th International Conference on Vibration Problems,* Lisbon, Portugal, 2013. pp. 1-10.